International Journal of Thermal Sciences 48 (2009) 1876–1883

Contents lists available at ScienceDirect

International Journal of Thermal Sciences

journal homepage: www.elsevier.com/locate/ijts

Free convection in a square cavity filled with a bidisperse porous medium

C. Revnic [a], T. Grosan [b], I. Pop [b,*], D.B. Ingham [c]

[a] Faculty of Pharmacy, University of Medicine and Pharmacy, Cluj-Napoca, Romania
[b] Babeş-Bolyai University, Applied Mathematics, R-3400 Cluj, CP 253, Romania
[c] Centre for Computational Fluid Dynamics, University of Leeds, Leeds LS2 9JT, UK

ARTICLE INFO

Article history:
Received 24 October 2008
Received in revised form
2 February 2009
Accepted 23 February 2009
Available online 14 March 2009

Keywords:
Free convection
Square cavity
Bidisperse porous medium
Numerical results

ABSTRACT

The classical problem of steady Darcy free convection in a square cavity filled with a porous medium has been extended to the case of a bidisperse porous medium (BDPM) by following the recent model proposed by Nield and Kuznetsov [D.A. Nield, A.V. Kuznetsov, Natural convection about a vertical plate embedded in a bidisperse porous medium, Int. J. Heat Mass Transfer 51 (2008) 1658–1664] and Rees et al. [D.A.S. Rees, D.A. Nield, A.V. Kuznetsov, Vertical free convective boundary-layer flow in a bidisperse porous medium, ASME J. Heat Transfer 130 (2008) 1–9]. The transformed partial differential equations in terms of the dimensionless stream function and temperature are solved numerically using a finite-difference method for some values of the governing parameters when the Rayleigh number Ra is equal to 10^2 and 10^3. Results are presented for the flow field with streamlines, temperature field by isotherms and heat transfer by local and mean Nusselt numbers are presented for both the f- and p-phases. It is found that the most important parameters that influence the fluid flow and heat transfer are the inter-phase heat transfer parameter H and the modified thermal conductivity ratio parameter γ.

1. Introduction

The problem of dealing with flow through a porous medium under the influence of temperature differences is one of the most considerable and contemporary subjects. This is because it finds many applications in geophysics, geothermal energy and technology, etc. The practical interest in convective heat transfer in porous media has greatly increased over the last several decades and this is due to the wide range of applications, such as thermal energy storage, geothermal energy utilization, petroleum reservoirs, chemical catalytic convectors, storage of grain, pollutant dispersion in aquifers, buried electrical cables, ceramic radiant porous burners used in industrial firms as efficient heat transfer devices, food industry, etc. The fundamental nature and the growing volume of work in this area are amply documented in the books by Nield and Bejan [1], Ingham and Pop [2], Vafai [3], Pop and Ingham [4], Bejan et al. [5], de Lemos [6] and Vadasz [7].

Recently, Nield and Kuznetsov [8], and Rees et al. [9] have considered the problem of steady free convection boundary layer flow over a vertical surface embedded in a bidisperse porous medium (BDPM). Also, these equations were applied by Nield and Kuznetsov [10,11] to forced convection in a channel and by Nield and Kuznetsov [12] to the Horton–Rogers–Lapwood problem (the paradigmatic problem for natural convection in an enclosed region). A very good description of the heat transport properties and basic equations of BDPM can be found in an excellent chapter by Nield and Kuznetsov [13] in the book by Ingham and Pop [2].

A bidisperse porous medium is composed of clusters of large particles that are agglomerations of small particles. Thus, a BDPM may be looked at as a standard porous medium in which the solid phase is replaced by another porous medium, whose temperature may be denoted by T_p if local thermal equilibrium is assumed within each cluster. We can then talk about the f-phase (the macropores) and the p-phase (the remainder of the structure). Therefore, in this paper attention will be focused on the steady free convection flow in a square enclosure filled with a bidisperse porous medium (BDPM). Constant temperatures are imposed along the vertical walls, while the upper and lower walls of the enclosure are assumed adiabatic. The dimensionless transport equations for continuity, momentum and energy are solved numerically. It is worth mentioning to this end that the classical problem of free convection flow in a square cavity filled with a standard porous medium (local thermal equilibrium, LTE) has been studied by many researchers, while that of a square cavity filled with a porous medium using the local thermal non-equilibrium (LTN) flow model has been studied by Baytas and Pop [14]. However, as it was pointed out by Nield and Kuznetsov [8] there is a significant lack of progress

* Corresponding author. Tel.: +40 264 594315; fax: +40 264 591906.
E-mail address: pop.ioan@yahoo.co.uk (I. Pop).

1290-0729/$ – see front matter © 2009 Elsevier Masson SAS. All rights reserved.
doi:10.1016/j.ijthermalsci.2009.02.016

Nomenclature

c	specific heat at constant pressure, J/kg K
g	acceleration due to gravity, m/s^2
G	negative of the applied pressure gradient, kg/m^2 s^2
h	inter-phase heat transfer coefficient (incorporating the specific area)
H	dimensionless inter-phase heat transfer parameter
k	thermal conductivity, W/m K
K	permeability, m^2
K_r	dimensionless permeability ratio parameter
L	width of the square cavity, m
Nu	local Nusselt number
$\overline{Nu}$	average Nusselt number
p	pressure, Pa
P	dimensionless pressure
q_w	wall heat flux, W/m^2
Ra	Rayleigh number for a porous medium
T	temperature, K
T_F	volume average of the temperature over the fluid, K
T_0	characteristic temperature, K
u	filtration velocity along x-axis, m/s
U	dimensionless velocity along X-axis
v	filtration velocity along y-axis, m/s
V	dimensionless velocity along Y-axis
x	coordinate measured along the lower horizontal wall, m
X	dimensionless coordinate in the horizontal direction
y	coordinate measured along the hot vertical wall, m
Y	dimensionless coordinate in the vertical direction

Greek symbols

β	dimensionless modified thermal capacity ratio
$\widehat{\beta}$	volumetric thermal expansion coefficient of the fluid, K^{-1}
ε	porosity within the p-phase
γ	dimensionless modified thermal conductivity ratio
ϕ	volume fraction of the f-phase
μ	fluid viscosity, kg/m s
θ	dimensionless temperature
ρ_F	density of the fluid, kg/m^3
σ_f	dimensionless f-phase momentum transfer parameter
ς	coefficient for momentum transfer between the two phases, kg/m^3 s
τ	dimensionless parameter

Subscripts

c	cold wall
f	fracture phase (macrophase)
h	hot wall
p	porous phase (micropores)

in the area of BDPM. To the best of our knowledge the present problem of free convection in a square cavity filled with a BDPM has not been considered before so that the presented results are new and original.

2. Basic equations

Consider the steady free convection flow and heat transfer inside a square cavity of width L which is filled with a BDPM porous medium as shown in Fig. 1. It is assumed that the temperature of the right hand wall of the cavity is T_h and the temperature of the left wall is T_c. Following Nield and Kuznetsov [8], we recognize that in a BDPM the fluid occupies all of the f-phase and a fraction of the p-phase. Thus, the basic equations for a BDPM are, see Nield and Kuznetsov [8],

$$\frac{\partial u_f}{\partial x}+\frac{\partial v_f}{\partial y}=0 \tag{1a}$$

$$\frac{\partial u_p}{\partial x}+\frac{\partial v_p}{\partial y}=0 \tag{1b}$$

$$T_F=\frac{\phi T_f+(1-\phi)\varepsilon T_p}{\phi+(1-\phi)\varepsilon} \tag{2}$$

$$\frac{\partial p}{\partial x}=-\frac{\mu}{K_f}u_f-\varsigma\left(u_f-u_p\right) \tag{3a}$$

$$\frac{\partial p}{\partial x}=-\frac{\mu}{K_p}u_p-\varsigma\left(u_p-u_f\right) \tag{3b}$$

$$\frac{\partial p}{\partial y}=-\frac{\mu}{K_f}v_f-\varsigma\left(v_f-v_p\right)+\rho_F g\widehat{\beta}(T_F-T_\infty) \tag{3c}$$

$$\frac{\partial p}{\partial y}=-\frac{\mu}{K_p}v_p-\varsigma\left(v_p-v_f\right)+\rho_F g\widehat{\beta}(T_F-T_\infty) \tag{3d}$$

$$\phi(\rho c)_f\mathbf{v}_f\cdot\nabla T_f=\phi k_f\nabla^2T_f+h\left(T_p-T_f\right) \tag{4a}$$

$$(1-\phi)(\rho c)_p\mathbf{v}_p\cdot\nabla T_p=(1-\phi)k_p\nabla^2T_p+h\left(T_f-T_p\right) \tag{4b}$$

where x is the coordinate measured along the lower wall of the cavity and y is the coordinate measured along the left hand wall of the cavity, u and v are the filtration velocity components along the x and y axes, respectively, $\mathbf{v}$ is the filtration velocity vector, T is the

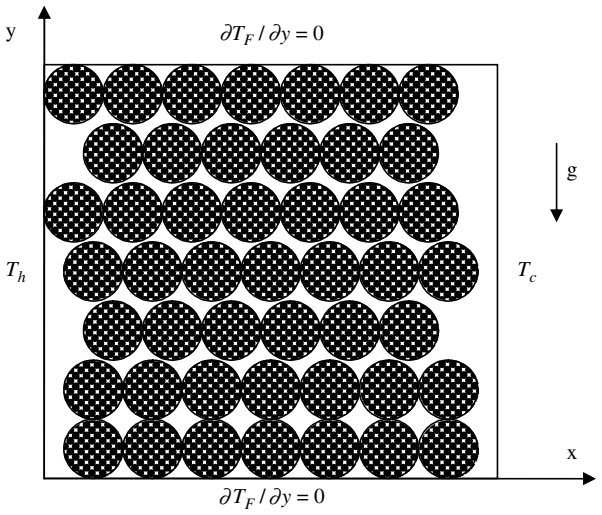

Fig. 1. Physical model and coordinate system.

temperature, p is the pressure, K is the permeability, g is the magnitude of the acceleration due to gravity, c is the specific heat at constant pressure, h is inter-phase heat transfer coefficient, ϕ is the volume fraction of the f-phase, μ is the dynamic viscosity, ρ_F is the fluid density, ς is the coefficient for momentum transfer between the two phases, ε is the porosity within the p-phase and $\widehat{\beta}$ is the volumetric thermal expansion coefficient of the fluid. The subscript f denotes the fracture phase (macropores) and p denotes the porous phase (micropores), respectively.

We define now the following dimensionless variables

$$(x,y) = L(X,Y), \quad \left(u_f, v_f\right) = \frac{k_f}{(\rho c)_f L}\left(U_f, V_f\right), \quad (u_p, v_p) = \frac{k_p}{(\rho c)_p L}(U_p, V_p) \quad p = \frac{k_f \mu}{(\rho c)_f K_f} P,$$
$$T_f = T_0 + (T_h - T_0)\theta_f, \quad T_p = T_0 + (T_h - T_0)\theta_p \tag{5}$$

where $T_0 = (T_h + T_c)/2$. Substituting (5) into Eqs. (1)–(4), we obtain the following dimensionless equations:

$$\frac{\partial U_f}{\partial X} + \frac{\partial V_f}{\partial Y} = 0 \tag{6a}$$

$$\frac{\partial U_p}{\partial X} + \frac{\partial V_p}{\partial Y} = 0 \tag{6b}$$

$$\frac{\partial \theta_F}{\partial X} = \tau \frac{\partial \theta_f}{\partial X} + (1-\tau)\frac{\partial \theta_p}{\partial X} \tag{7}$$

$$\frac{\partial P}{\partial X} = -\left(1+\sigma_f\right)U_f + \sigma_f \beta U_p \tag{8a}$$

$$\frac{\partial P}{\partial X} = -\beta\left(\sigma_f + \frac{1}{K_r}\right)U_p + \sigma_f U_f \tag{8b}$$

$$\frac{\partial P}{\partial Y} = -\left(1+\sigma_f\right)V_f + \sigma_f \beta V_p + Ra\theta_F \tag{8c}$$

$$\frac{\partial P}{\partial Y} = -\beta\left(\sigma_f + \frac{1}{K_r}\right)V_p + \sigma_f V_f + Ra\theta_F \tag{8d}$$

$$\nabla^2 \theta_f = \phi\left(U_f \frac{\partial \theta_f}{\partial X} + V_f \frac{\partial \theta_f}{\partial Y}\right) + H\left(\theta_f - \theta_p\right) \tag{9a}$$

$$\nabla^2 \theta_p = (1-\phi)\left(U_p \frac{\partial \theta_p}{\partial X} + V_p \frac{\partial \theta_p}{\partial Y}\right) + \gamma H\left(\theta_p - \theta_f\right) \tag{9b}$$

where Ra is the Rayleigh number for a porous medium, σ_f is the f-phase momentum parameter, K_r is the permeability ratio, H is the dimensionless interface-phase heat transfer parameter, γ is the modified thermal conductivity ratio, β is the modified thermal capacity ratio and τ is a dimensionless parameter and they are defined as follows:

$$Ra = \frac{\rho_F g K_f \tilde{\beta}(T_h - T_0)L}{\mu \phi k_f/(\rho c)_f}, \quad \sigma_f = \frac{\varsigma K_f}{\mu}, \quad \beta = \frac{(1-\phi)k_p(\rho c)_f}{\phi k_f (\rho c)_p}$$
$$K_r = \frac{K_p}{K_f}, \quad H = \frac{hL^2}{\phi k_f}, \quad \gamma = \frac{\phi k_f}{(1-\phi)k_p}, \quad \tau = \frac{\phi}{\phi + (1-\phi)\varepsilon} \tag{10}$$

Further, we introduce the stream functions ψ_f and ψ_p defined in the usual way as follows:

Table 1
Accuracy test for $Ra = 10^3$, $H = 1$, $\gamma = 1$, $\sigma_f = 1$, $\beta = 10$, $\tau = 0.625$, $K_r = 0.001$ and $\phi = 0.5$.

Nodes	$\psi_f(0.25, 0.25)$	$\psi_p(0.25, 0.25)$	$\theta_f(0.25, 0.25)$	$\theta_p(0.25, 0.25)$
21×21	−14.7609	−0.0044	−0.2069	0.2331
41×41	−15.1395	−0.0045	−0.2101	0.2328
81×81	−15.2400	−0.0046	−0.2114	0.2328
161×161	−15.2583	−0.0046	−0.2121	0.2327
Richardson extrapolation	−15.2644	−0.0046	−0.2123	0.2328

$$U_f = \frac{\partial \psi_f}{\partial Y}, \quad V_f = -\frac{\partial \psi_f}{\partial X} \tag{11a}$$

$$U_p = \frac{\partial \psi_p}{\partial Y}, \quad V_p = -\frac{\partial \psi_p}{\partial X} \tag{11b}$$

Eliminating the pressure P from Eqs. (8) and using (11), we obtain

$$\left(1+\sigma_f\right)\nabla^2 \psi_f - \sigma_f \beta \nabla^2 \psi_p = -Ra\left[\tau \frac{\partial \theta_f}{\partial X} + (1-\tau)\frac{\partial \theta_p}{\partial X}\right] \tag{12a}$$

$$\beta\left(\sigma_f + \frac{1}{K_r}\right)\nabla^2 \psi_p - \sigma_f \nabla^2 \psi_f = -Ra\left[\tau \frac{\partial \theta_f}{\partial X} + (1-\tau)\frac{\partial \theta_p}{\partial X}\right] \tag{12b}$$

$$\nabla^2 \theta_f = \phi\left(\frac{\partial \psi_f}{\partial Y}\frac{\partial \theta_f}{\partial X} - \frac{\partial \psi_f}{\partial X}\frac{\partial \theta_f}{\partial Y}\right) + H\left(\theta_f - \theta_p\right) \tag{13a}$$

$$\nabla^2 \theta_p = (1-\phi)\left(\frac{\partial \psi_p}{\partial Y}\frac{\partial \theta_p}{\partial X} - \frac{\partial \psi_p}{\partial X}\frac{\partial \theta_p}{\partial Y}\right) + \gamma H\left(\theta_p - \theta_f\right) \tag{13b}$$

which are subject to the boundary conditions

$$\begin{aligned} &\psi_f = 0,\ \psi_p = 0,\ \theta_f = \frac{1}{2},\ \theta_p = \frac{1}{2} \quad at\ X = 0 \\ &\psi_f = 0,\ \psi_p = 0,\ \theta_f = -\frac{1}{2},\ \theta_p = -\frac{1}{2} \quad at\ X = 1 \\ &\psi_f = 0,\ \psi_p = 0,\ \frac{\partial \theta_f}{\partial Y} = 0,\ \frac{\partial \theta_p}{\partial Y} = 0 \quad at\ Y = 0\ and\ Y = 1 \end{aligned} \tag{14}$$

The physical quantities of interest are the local Nusselt numbers Nu_f of the f-phase (fracture phase) and Nu_p of the p-phase (porous phase), respectively, at the hot wall which are defined as follows:

$$Nu_f = \frac{Lq_{wf}}{k_f(T_w - T_0)}, \quad Nu_p = \frac{Lq_{wp}}{k_p(T_w - T_0)} \tag{15}$$

where q_{wf} and q_{wp} are the heat fluxes of the f- and p-phases at the hot wall and which are given by

Table 2
Comparison of the mean Nusselt number $\overline{Nu}$ for a square cavity filled with a regular (monodisperse, $\theta_f = \theta_p$) porous medium with results from the open literature at $Ra = 10^3$.

References	$\overline{Nu}$
Bejan [16]	15.800
Cross et al. [17]	13.470
Goyeau et al. [18]	13.470
Baytas and Pop [19]	14.060
Saeid and Pop [20]	13.726
Manole and Lage [21]	13.637
Varol et al. [22]	13.564
Present	13.664 (13.754, Richardson extrapolation)

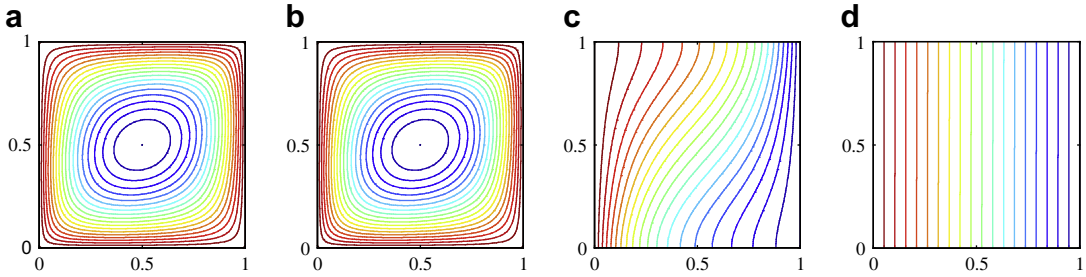

Fig. 2. Streamlines (a and b) and isotherms (c and d) for $Ra = 10^2$, $H = 0.05$, $\gamma = 1$.

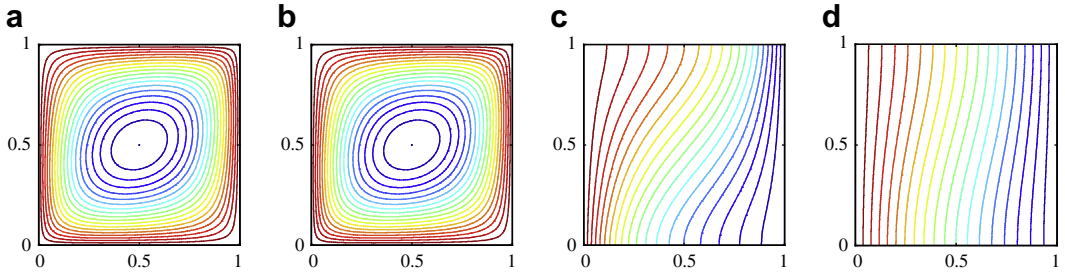

Fig. 3. Streamlines (a and b) and isotherms (c and d) for $Ra = 10^2$, $H = 1$, $\gamma = 10$: (a, c) f-phase and (b, d) p-phase.

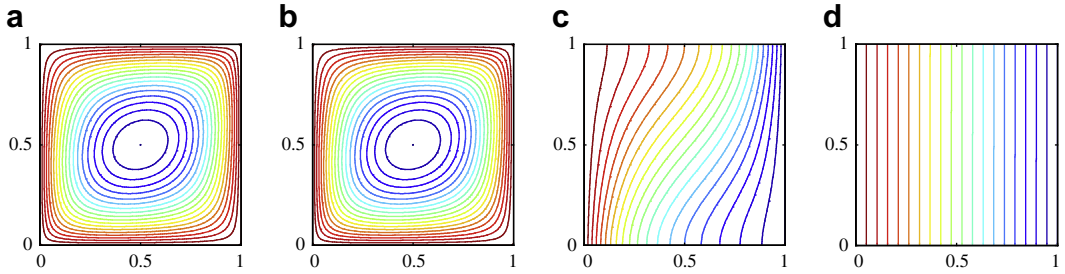

Fig. 4. Streamlines (a and b) and isotherms (c and d) for $Ra = 10^2$, $H = 1$, $\gamma = 0.01$: (a, c) f-phase and (b, d) p-phase.

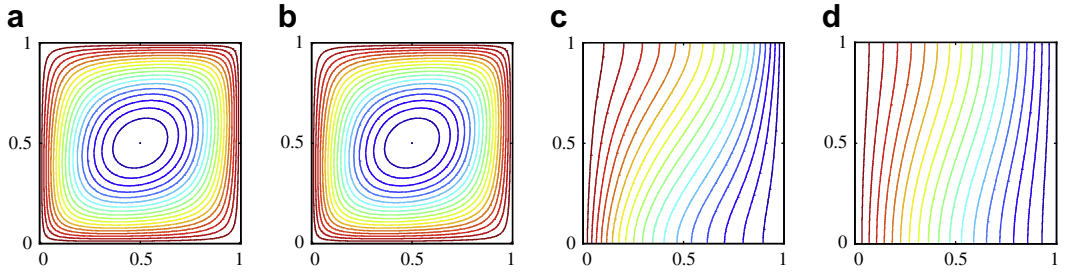

Fig. 5. Streamlines (a and b) and isotherms (c and d) for $Ra = 10^2$, $H = 10$, $\gamma = 2$: (a, c) f-phase and (b, d) p-phase.

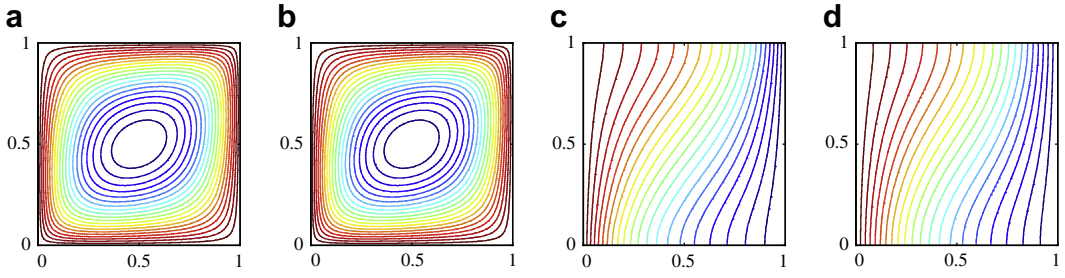

Fig. 6. Streamlines (a and b) and isotherms (c and d) for $Ra = 10^2$, $H = 10$, $\gamma = 10$: (a, c) f-phase and (b, d) p-phase.

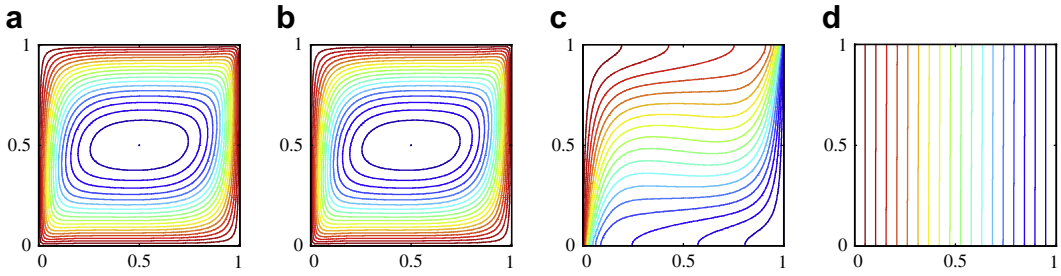

Fig. 7. Streamlines (a and b) and isotherms (c and d) for $Ra = 10^3$, $\gamma = 1$, $H = 0.05$: (a, c) f-phase and (b, d) p-phase.

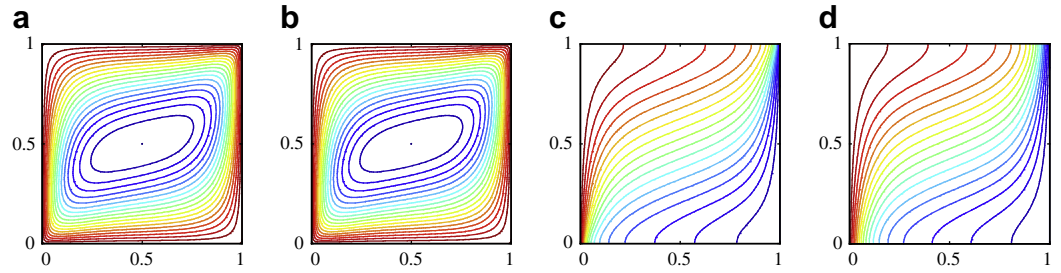

Fig. 8. Streamlines (a and b) and isotherms (c and d) for $Ra = 10^3$, $\gamma = 1$, $H = 500$: (a, c) f-phase and (b, d) p-phase.

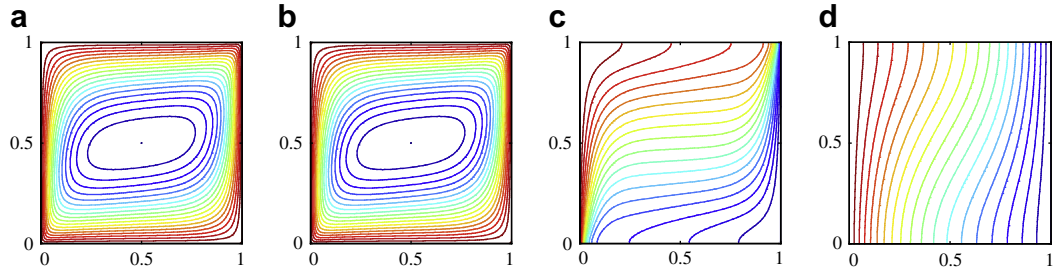

Fig. 9. Streamlines (a and b) and isotherms (c and d) for $Ra = 10^3$, $\gamma = 10$, $H = 1$: (a, c) f-phase and (b, d) p-phase.

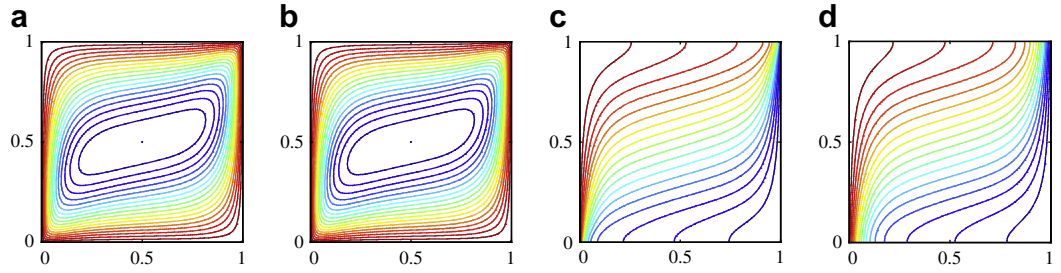

Fig. 10. Streamlines (a and b) and isotherms (c and d) for $Ra = 10^3$, $\gamma = 10$, $H = 50$: (a, c) f-phase and (b, d) p-phase.

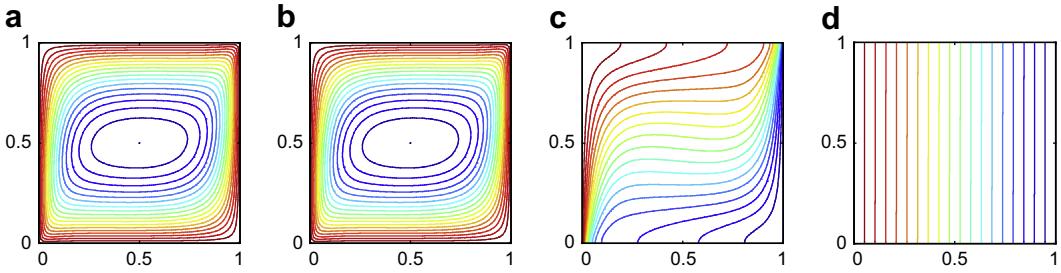

Fig. 11. Streamlines (a and b) and isotherms (c and d) for $Ra = 10^3$, $H = 1$, $\gamma = 0.01$: (a, c) f-phase and (b, d) p-phase.

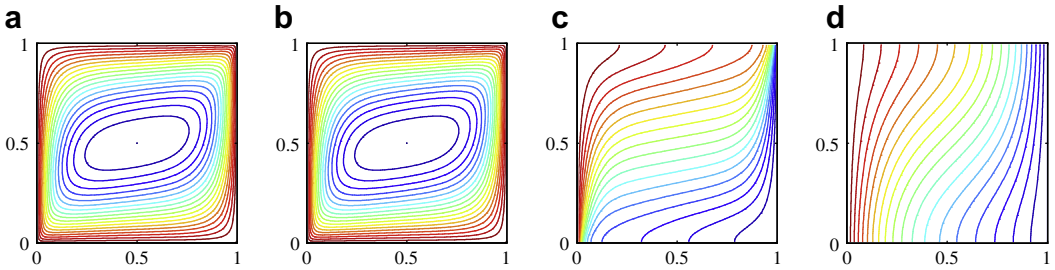

Fig. 12. Streamlines (a and b) and isotherms (c and d) for $Ra = 10^3$, $H = 10$, $\gamma = 2$: (a, c) f-phase and (b, d) p-phase.

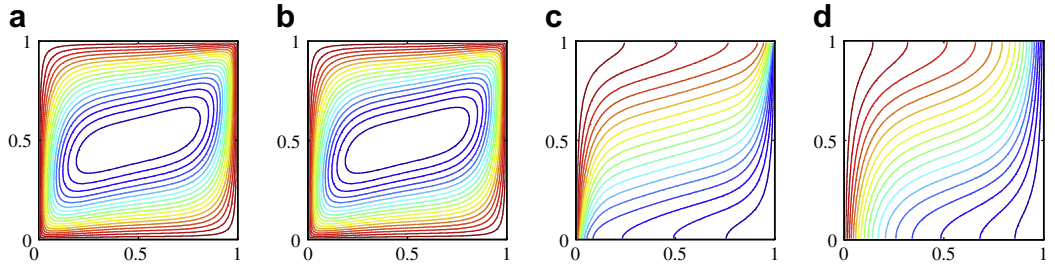

Fig. 13. Streamlines (a and b) and isotherms (c and d) for $Ra = 10^3$, $H = 10$, $\gamma = 10$: (a, c) f-phase and (b, d) p-phase.

$$q_{wf} = -k_f\left(\frac{\partial T_f}{\partial x}\right)_{x=0}, \quad q_{wp} = -k_p\left(\frac{\partial T_p}{\partial x}\right)_{x=0} \tag{16}$$

Using variables from (5), we then obtain from (15) and (16)

$$Nu_f = -\left(\frac{\partial \theta_f}{\partial X}\right)_{X=0}, \quad Nu_p = -\left(\frac{\partial \theta_p}{\partial X}\right)_{X=0} \tag{17}$$

The mean Nusselt numbers of the f- and p-phases from the heated wall are given by

$$\overline{Nu}_f = \int_0^1 Nu_f \, dY, \quad \overline{Nu}_p = \int_0^1 Nu_p \, dY \tag{18}$$

3. Numerical method

To obtain the numerical solution of Eqs. (12) and (13) a central finite-difference scheme was used and the system of discretized equations has been solved using a Gauss–Seidel iteration technique. The unknowns ψ and θ were calculated iteratively until the following criterion of convergence was fulfilled

$$\sum_{i,j}|\chi_{new}(i,j) - \chi_{old}(i,j)| / \sum_{i,j}|\chi_{new}(i,j)| \le \varepsilon \tag{19}$$

whereχ represents the temperature or the stream function and ε is the convergence criterion. In all the results presented in this paper, $\varepsilon = 10^{-7}$ was found to be sufficiently small such that any smaller value produced results which were graphically the same. In order to choose the size of the grid, accuracy tests using the finite-difference method and Richardson extrapolation [15] for mesh sensitivity analysis were performed for $Ra = 10^3$ using four sets of grids: 21×21, 41×41, 81×81 and 161×161 as shown in Table 1. Reasonably good agreement was found between the 81×81 and 161×161 grids and therefore the grid used in this problem was 81×81 and these give accurate results for the values of Ra considered. Due to lack of suitable results in the literature pertaining to the present configuration, the obtained numerical results have been validated against the existing results for the case of natural convection heat transfer problem in a differentially heated square cavity filled with a regular (monodisperse) porous medium (the case $\sigma_f = 0$, $K_r = 0$, $\tau = 1$, $\theta_f = \theta_p$ and $\phi = 1$). The obtained numerical results for the average Nusselt number $\overline{Nu}_f = \overline{Nu}_p = \overline{Nu}$ are compared in Table 2 with those given by different authors from the open literature. As it can be seen the obtained result shows good agreement with the results reported by the mentioned authors.

Also, in rectangular enclosures, contours of streamlines and isotherms are almost the same as the ones given in the literature. However, these results are not presented here in order to save space. The same algorithm as that used in the present paper was recently tested for the problem of natural convection in a rectangular enclosure filled with a regular (monodisperse) porous medium under the influence of an inclined magnetic field by Grosan et al. [23]. Therefore, we are confident that the results reported in the present paper are accurate.

4. Results and discussions

Steady natural convection in a square cavity filled with a bidisperse porous medium (BDPM) has been numerically studied for the value of the Rayleigh number $Ra = 10^2$ and 10^3. The values of the parameters β – the modified thermal capacity ratio, σ_f – the f-phase momentum transfer, permeability ratio parameter K_r and τ are $\beta = 10$, $\sigma_f = 1.0$, $K_r = 0.001$, $\tau = 0.625$. We consider the value of $\phi = 0.5$, which corresponds to the sand [24] while the values of modified thermal conductivity ratio parameter γ and inter-phase heat transfer parameter H vary in the ranges $0 \le \gamma \le 10$ and $0 \le H \le 500$. We mention that the values of the parameters β, σ_f, K_r and τ are those considered by Nield and Kuznetsov [8], and Rees et al. [9]. However, only small values of the parameters σ_f, K_r and τ were considered as this is the situation that usually exists in geophysical and engineering applications. The results for the flow field with streamlines, temperature field by isotherms and heat transfer by local and mean Nusselt numbers are presented for both the f- and p-phases in Figs. 2–15. Figs. 2–6 show streamlines (on the

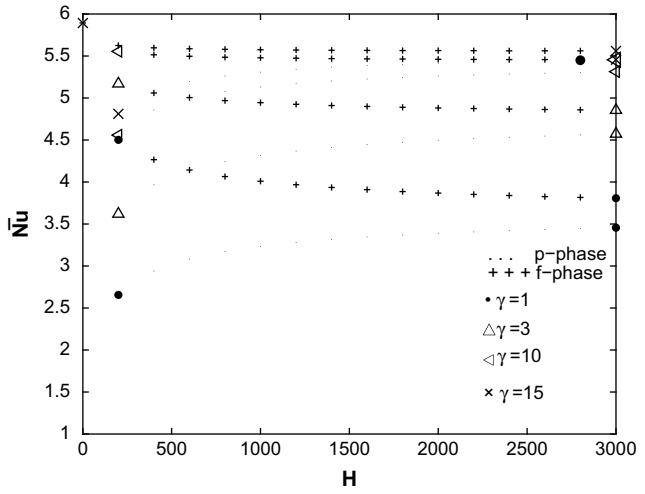

Fig. 14. Variation of the mean Nusselt numbers with H for some values of γ.

left) and isotherms (on the right) for $Ra = 10^2$ and Figs. 7–13 show results for $Ra = 10^3$. Figs. 14 and 15 illustrate results for the Nusselt number. It can be observed that for the value of Ra considered, the flow is unicellular and isotherms are almost parallel to each other. In addition, a nearly centrally located cell is observed. For small values of γ isotherms are nearly parallel with the walls of the cavity and this exhibits nearly pure conduction characteristics. However, for larger values of H and γ the effect of convection also influences the flow, that is, the distributions of the isotherms are not parallel with the walls of the cavity. From the distribution of streamlines in Figs. 7–13, a boundary layer type of flow is observed at $Ra = 10^3$ on both vertical walls. From the distribution of isotherms for the same Ra, on the other hand, thermal boundary layer is observed on vertical walls.

Further, Figs. 14 and 15 illustrate the variation of the mean Nusselt numbers of the f- and p-phases from the heated wall of the cavity, $\overline{Nu}_f$ and $\overline{Nu}_p$, with the parameters H and γ for $Ra = 10^3$, $\beta = 10, \sigma_f = 1.0, K_r = 0.001, \tau = 0.625$ and $\phi = 0.5$. It is seen from these figures that similar to the case of the local thermal non-equilibrium (LTNE) model, for a bidisperse porous medium there is also a substantial difference between the heat transfer rates of the f- and p-phases when values of H and γ are small. This is not surprising

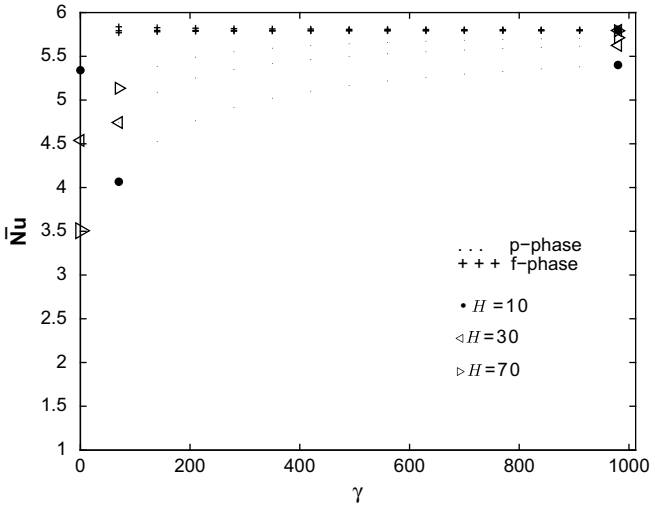

Fig. 15. Variation of the mean Nusselt numbers with γ for some values of H.

since H is a measure of the way in which heat is transferred between the phases and γ is a measure of thermal conductivity ratio between the phases. As H and γ increase, the heat transfer between the f- and p-phases occurs more rapidly and this is reflected by the increasing similarity between the heat transfer rates and thermal conductivity of the two phases. Thus, large values of H and γ reduce the non-equilibrium effects. However, for small values of H and γ the values of $\overline{Nu}_p$ are much lower than those of $\overline{Nu}_f$.

Finally, it is worth noticing that the present results for the BDPM illustrated in these figures show the general trend of those presented by Baytas and Pop [19] for the local thermally non-equilibrium (LTNE) model.

5. Conclusions

The present paper extends the classical problem of steady Darcy free convection in a square cavity filled with a porous medium to the case of a bidisperse porous medium (BDPM) by following the recent model proposed by Nield and Kuznetsov [8] and Rees et al. [9]. The transformed partial differential equations in terms of the dimensionless stream function and temperature are solved numerically using a finite-difference method for some values of the governing parameters when the Rayleigh number Ra is equal to 10^2 and 10^3, respectively. The numerical results illustrate features concerning the effects of a modified thermal capacity ratio parameter, the f-phase momentum transfer parameter, permeability ratio parameter,τ, modified thermal conductivity ratio parameter γ and inter-phase heat transfer parameter H. Detailed results for the flow field, temperature distribution and heat transfer rates have been presented in terms of streamlines, isotherms and mean Nusselt number. The main conclusions of the present analysis are as follows:

- the conduction is the dominant mode of heat transfer when the values of Ra increase from 10^2 to 10^3 and the convection effect influences the flow when the values of H and γ increase,
- the dimension of the central cells increases with the increase of Ra, and
- the orientation of the central cells changes with the values of H and γ.

Finally, it should be pointed out that a number of aspects that could form the subject of further studies of this problem can be raised as those mentioned by Nield and Kuznetsov [8], and Rees et al. [10] in the section 'Conclusions' of their papers. Thus, it appears that the number of parameters in the present analysis cannot be reduced beyond 7. From our numerical procedure it was not possible to solve Eqs. (12)–(14) for any values of the governing parameters. Therefore, we are confident that the BDPM system is a distinctive system that is well worth further study. As far as we are aware, there are only just a few published papers on the BDPM model.

Acknowledgements

C. Revnic and T. Grosan wish to thank the UEFISCSU Grant PN-II-ID 525/2007. The authors would like to express their very sincere thanks to reviewers for their valuable comments and suggestions.

References

[1] D.A. Nield, A. Bejan, Convection in Porous Media, third ed. Springer, New York, 2006.
[2] D.B. Ingham, I. Pop (Eds.), Transport Phenomena in Porous Media, Elsevier, Oxford, 2005.

[3] K. Vafai (Ed.), Handbook of Porous Media, second ed. Taylor & Francis, Boca Raton, 2005.
[4] I. Pop, D.B. Ingham, Convective Heat Transfer: Mathematical and Computational Modelling of Viscous Fluids and Porous Media, Pergamon, Oxford, 2001.
[5] A. Bejan, I. Dincer, S. Lorente, A.F. Miguel, A.H. Reis, Porous and Complex Flow Structures in Modern Technologies, Springer, New York, 2004.
[6] M.J.S. de Lemos, Turbulence in Porous Media: Modeling and Applications, Elsevier, Oxford, 2006.
[7] P. Vadasz (Ed.), Emerging Topics in Heat and Mass Transfer in Porous Media, Springer, New York, 2008.
[8] D.A. Nield, A.V. Kuznetsov, Natural convection about a vertical plate embedded in a bidisperse porous medium, Int. J. Heat Mass Transfer 51 (2008) 1658–1664.
[9] D.A.S. Rees, D.A. Nield, A.V. Kuznetsov, Vertical free convective boundary-layer flow in a bidisperse porous medium, ASME J. Heat Transfer 130 (2008) 1–9.
[10] D.A. Nield, A.V. Kuznetsov, Forced convection in a bi-disperse porous medium channel: a conjugate problem, Int. J. Heat Mass Transfer 47 (2004) 5375–5380.
[11] D.A. Nield, A.V. Kuznetsov, A two-velocity two-temperature model for a bi-dispersed porous medium: forced convection in a channel, Transport Porous Med. 59 (2005) 325–339.
[12] D.A. Nield, A.V. Kuznetsov, The onset of convection in a bidisperse porous medium, Int. J. Heat Mass Transfer 49 (2006) 3068–3074.
[13] D.A. Nield, A.V. Kuznetsov, Heat transfer in disperse porous media, in: D.B. Ingham, I. Pop (Eds.), Transport Phenomena in Porous Media III, Elsevier, Oxford, 2005.
[14] A.C. Baytas, I. Pop, Free convection in a square cavity using a thermal nonequilibrium model, Int. J. Thermal Sci. 41 (2002) 861–870.
[15] G.D. Smith, Numerical Solution of Partial Differential Equations. Finite Difference Method, Oxford University Press, Oxford, 2004.
[16] A. Bejan, On the boundary layer regime in a vertical enclosure filled with a porous medium, Lett. Heat Mass Transfer 6 (1979) 93–102.
[17] R.J. Cross, M.R. Bear, C.E. Hickox, The application of flux-corrected transport (FCT) to high Rayleigh number natural convection in a porous medium, in: Proceedings of 8th International Heat Transfer Conference, San Francisco, 1986.
[18] B. Goyeau, J.P. Songbe, D. Gobin, Numerical study of double-diffusive natural convection in a porous cavity using the Darcy–Brinkman formulation, Int. J. Heat Mass Transfer 39 (1996) 1363–1378.
[19] A.C. Baytas, I. Pop, Natural convection in a trapezoidal enclosure filled with a porous medium, Int. J. Eng. Sci. 39 (2001) 125–134.
[20] N.H. Saeid, I. Pop, Natural convection from a discrete heater in a square cavity filled with a porous medium, J. Porous Med. 8 (2005) 55–63.
[21] D.M. Manole, J.L. Lage, Numerical benchmark results for natural convection in a porous medium cavity, in: ASME Heat Mass Transfer Porous Med. Conf., 1992, pp. 55–60.
[22] Y. Varol, H.F. Oztop, I. Pop, Influence of inclination angle on buoyancy-driven convection in triangular enclosure filled with a fluid-saturated porous medium, Heat Mass Transfer 44 (2008) 617–624.
[23] T. Grosan, C. Revnic, I. Pop, D.B. Ingham, Magnetic field and internal heat generation effects on the free convection in a rectangular cavity filled with a porous medium, Int. J. Heat Mass Transfer 52 (2009) 1525–1533.
[24] A. Bejan, J.L. Lage, Heat transfer from a surface covered with hair, in: S. Kakaç, B. Kilkis, F.A. Kulacki, F. Arinç (Eds.), Convective Heat and Mass Transfer in Porous Media, Kluwer, Dordrecht, 1991.